Check for updates

Proceedings of the 2020 Design of Medical Devices Conference
DMD2020
April 6, 7-9, 2020, Minneapolis, MN, USA

DMD2020-9060

Downloaded from https://proceedings.asmedigitalcollection.asme.org/BIOMED/proceedings-pdf/DMD2020/83549/V001T07A005/6552792/v001t07a005-dmd2020-9060.pdf by guest on 28 July 2020

A PRECISE SCALE-UP METHOD TO PREDICT PARTICLE DELIVERED DOSE IN A HUMAN RESPIRATORY SYSTEM USING RAT DEPOSITION DATA: AN IN SILICO STUDY

Hamideh Hayati, Yu Feng[1]
School of Chemical Engineering, Oklahoma State University, Stillwater, OK 74078, USA

ABSTRACT

As surrogates to human beings, rats are used occasionally to study the therapeutic impact of inhaled pulmonary drug particles in microscale. To speculate human responses from rat studies, scale-up factors are widely used to extrapolate particle lung deposition from rat to human. However, available scale-up methods are highly simplified and not accurate, because they directly use the human-to-rat ratios of body weights (RBW) or lung surface areas (RSA) as the scale-up factor. To find a precise scale-up strategy, an experimentally validated Computational Fluid-Particle Dynamics (CFPD) was employed to simulate the transport and deposition of microparticles in both human and rate respiratory systems, which encompasses the pulmonary routes from mouth/nose to airways up to Generation 17 (G17) for human and G23 for the rat. Microparticles with the same range of Stk/Fr were injected into both models with the airflow at resting conditions. Numerical results indicate that particles (with the size ranging from 1 to 13 μm for humans and 0.6 to 6 μm for rat) have similar deposition pattern (DP) and deposition fraction (DF) in both models, which are resulted from both inertial impaction and gravitational sedimentation effects. A novel correlation is proposed to predict DFs in both human and rat respiratory systems as a function of the ratio of Stokes number to Froude number (Stk/Fr). Using the correlation as the novel scale-up tool, inter-species extrapolations can be precisely done on predicting particle depositions in human respiratory systems based on the deposition data in rats obtained from animal studies.

Keywords: A Rat-to-Human Scale-up Method; Computational Fluid-Particle Dynamics (CFPD); Respiratory System

NOMENCLATURE

Acronym	
BC	Boundary condition
CFPD	Computational fluid-particle dynamics
CT	Computed Tomography
D_{in}	Inlet hydraulic diameter
DF	Deposition fraction
DP	Deposition pattern
Fr	Froude number
G	Generation
g	Gravitational acceleration
m	Particle mass
RBW	Ratio of body weights
RSA	Ratio of lung surface areas
Stk	Stokes number
T	Trachea
TB	Tracheobronchial tree
t	Time
UA	Upper airway
UDF	User-defined function
v	Velocity
Greek symbols	
ρ	Air density
μ	Air viscosity
Subscripts	
p	Particle
Superscripts	
BM	Brownian motion
D	Drag
G	Gravity
L	Lift
p	Particle

[1] Contact author: yu.feng@okstate.edu

Copyright © 2020 ASME

BACKGROUND

Rats are frequently used in preclinical trials of pulmonary healthcare research with aerosolized drug designs to predict human responses [1]. However, research has demonstrated that the widely used scale-up methods are not precise for the estimation of particle depositions in human respiratory systems from rat studies [2]. Specifically, neglecting the anatomical feature differences of the respiratory systems between human and rat, using the rat-to-human ratio of BWs, airway volumes or surface areas as the scale-up factors are not accurate. To incorporate the airway morphology effect on the particle deposition into the scale-up methodology as a more precise procedure, the particle transport and deposition in both human and rat respiratory systems need to be quantified using the experimentally validated CFPD model [3]. For microparticles, inertial impaction and interception are both important for the deposition. The gravitational sedimentation will also compensate for the dominance of inertia as the particle diameter increases [3, 4]. Specifically, Xi et al. [3] conducted an intra-species particle deposition study using three rat nasal cavities with different scales. They injected microparticles of sizes of 4,8, and 12 μm into scaled-up models with scaling factors 1, 2, and 3, respectively, while the Stokes numbers (Stk) were kept the same. They observed the particles followed a similar DP in different scaled-up models. They also found that depositions of larger particles are not only dominated by the inertial impaction, but also by the gravitational sedimentation effect characterized by the Froude number (Fr). Another study [4] analyzed the inertial and gravitational deposition of microparticles in a triple bifurcation representing G6 to G9 human airways. Based on the findings in the existing papers [3, 4], the central hypothesis of this study is introduced and validated, that microparticles with the same Stk/Fr will have the same deposition fractions (DFs) in upper airways and the tracheobronchial trees of both human and rat. By predicting the DFs of particles with different sizes and Stk/Fr values using the experimentally validated CFPD model [5, 6], correlations were generated for the DF as a function of Stk/Fr with good consistency between the particle depositions in human and rat.

METHODOLOGY

A one-way coupled Euler-Lagrange method was employed to model the particle-laden airflow transport phenomena and predict the particle depositions in both human and rat respiratory systems. The Euler-Lagrange method employed in this study was enhanced by in-house C and MATLAB programs.

1.1 Geometries and Meshes

The human and rat airway configurations were adopted from [7] and [8], respectively. The original version of the human airway consisted of the extrathoracic airway and tracheobronchial (TB) tree up to G9, which later was extended up to G17. The current model has a total surface area of 1.34e-1 m^2 and it consists of the upper airway (nasal cavity, larynx, and pharynx), trachea, and the tracheobronchial tree from G0 to G17. The scanned data was obtained from a 47-year old healthy male whose body weight is 74 kg (see Fig. 1 (a)). The rat airway model with a total surface area of 2.72e-3 m^2 is shown in Fig. 1 (b), and contains the upper airway, trachea, and tracheobronchial tree from G0 to G23. The rate airway was reconstructed from a 9 to 10 weeks old Sprague Dawley (S-D) rat of which the bodyweight is 300 g.

Using ANSYS Fluent Meshing (ANSYS Inc., Canonsburg, PA), the computational domain of the human airway model was discretized into 7,064,092 polyhedral elements, while for the rat model it was 11,741,105 polyhedrons. For both geometries, 5 near-wall prism layers were generated to resolve the boundary layer and capture laminar-to-turbulence transitions near the walls precisely.

1.2 Governing Equations

For solving the governing equations of the continuous flow field for both the human and the rat, the Transition Shear-Stress Transport (SST) turbulence model [9] was applied. Since the inlet boundary conditions of breathing flow rates for both human and rat are unsteady and have both acceleration and deceleration phases, the averaged inlet airflow velocity ranges from 0 to 5.8 m/s and 2.6 m/s, respectively. Accordingly, the maximum Reynolds number (Re) in the human respiratory system is 2,484, indicating that the laminar-to-turbulence transition regime exists. In addition, the maximum Re in the rate respiratory system is 1,122. The transition from laminar to turbulence may occur at Re=2000 for steady flow in a straight tube. Based on the maximum Re in the respiratory systems, transitional flow regimes can be found in the upper airway and the turbulence will be re-laminarized as the air transport deeper to the tracheobronchial trees [10]. Based on the laminar-to-turbulence flow regime, the previous validated Transition Shear-Stress Transport (SST) model was employed [5, 6].

For tracking the microparticles, a Lagrangian method was applied. Assuming particles are spherical and neglecting the thermophoretic force, the translational equation for each particle can be given by [6, 11]:

$$\frac{d}{dt}(m_i u_i{}^p) = F_i{}^D + F_i{}^L + F_i{}^{BM} + F_i{}^G \quad (1)$$

where m_i and $u_i{}^p$ are the particle mass and velocity, respectively. $F_i{}^D$ denotes the drag force, $F_i{}^L$ is the Saffman lift force [12], $F_i{}^{BM}$ is the Brownian motion induced force [5], and $F_i{}^G$ represents gravity. In addition, to quantify the regional deposition in respiratory systems, the regional deposition fraction (DF) is employed and defined as:

$$DF = \frac{Number\ of\ deposited\ particles\ in\ a\ specific\ region}{Number\ of\ particles\ entering\ the\ nose} \quad (2)$$

1.3 Numerical Setup

ANSYS Fluent 19.2 (ANSYS Inc., Canonsburg, PA) was used to simulate the lung aerosol dynamics in both human and rat airway models. For both airway models, the same types of boundary conditions (BCs) were applied. For example, the pressure outlet BCs were assigned to the airway outlets and non-slip velocity BCs were applied on airway walls. Specifically, the realistic transient breathing waveform for the human was employed [13, 14]. For the rat, an idealized

Downloaded from https://proceedings.asmedigitalcollection.asme.org/BIOMED/proceedings-pdf/DMD2020/83549/V001T07A005/6552792/v001t07a005-dmd2020-9060.pdf by guest on 28 July 2020

 Copyright © 2020 ASME

sinusoidal breathing waveform was used [13]. Both waveforms represent breathing patterns at rest for the human and the rat, respectively. For both airway models, the airflow initiated from the nostrils, along which the particles were injected with a uniform distribution. The breathing waveforms and the particle diameter ranges selected in this study are shown in Fig. 1 and Table 1. The average inlet velocities are 5.3 m/s and 1.7 m/s for human and rat, respectively. Particles were injected after one breathing cycle for both human and rat, in order to have realistic initial airflow fields. For both human and rat airway models, the flow time steps are 0.02 s. Particle tracking for all the particle sizes was executed within one breathing cycle.

Additionally, in-house user-defined functions (UDFs) were developed and compiled for:

(1) Specifying transient inhalation and exhalation profiles at the nostrils;
(2) Recovering the anisotropic corrections on turbulence fluctuation velocities; and
(3) Modeling the Brownian motion induced forces on particles.

Furthermore, numerical simulations were performed on a local Dell Precision T7810 workstation (Intel® Xeon® Processor E5-2643 v4 with dual processors, 64 cores and 128 GB RAM) and a local Dell Precision T7910 workstation (Intel®Xeon® Processor E5-2683 v4 with dual processors, 64 cores, and 256 GB RAM). Using 32 cores, it took approximately 9 hours (particles of d_p=9 µm for human airway) to 648 hours (particles with d_p=1 µm for rat airway) to complete one simulation.

RESULTS AND DISCUSSION

2.1 Airflow Structures

Both human and rat nasal cavities have complex airflow passages, which causes the airflow to accelerate immediately when it enters the nasal cavity through nostrils. However, because of the sharper turns along the routes of rat nasal vestibule, the airflow velocity in the rat nasal cavity increases more rapidly than in the human nasal cavity [15]. It can be observed that the airflow velocity increases up to 4.5 times the inlet velocity in the rat nasal vestibule, while it increases up to 1.4 in the human nasal cavity. The above-mentioned morphological differences between rat and human nasal cavities and the induced velocity field variations make the rat nasal cavity a better filtration system to trap microparticles.

2.2 Localized Particle Deposition Patterns

Local deposition patterns of particles with different aerodynamic diameters are displayed in Figs. 1 (a) and (b). The effects of the airway morphology and particle diameter (d_p) on the DP can be observed. The range of d_p was selected based on their corresponding inlet Stokes number (Stk) [3], which are presented in Table 1.

The DPs shown in Figs. 1 (a) and (b) indicate that large particles, i.e., d_p>10µm (Stk>6E-1) for human and d_p>5µm (Stk>7E-1) for the rat, accumulated at several "hot spots", such as the rat nasal vestibule and human olfactory, superior, and middle turbinate regions. It can be also observed that the DPs become more uniformly distributed when the particle size decreases.

TABLE 1. PARTICLE AERODYNAMIC DIAMETERS AND THE CORRESPONDING STOKES NUMBERS

Rat model		Human model	
d_p (µm)	Stk	d_p(µm)	Stk
0.6	2.00E-2	1	6.05E-3
6	1.34E+0	13	8.34E-1

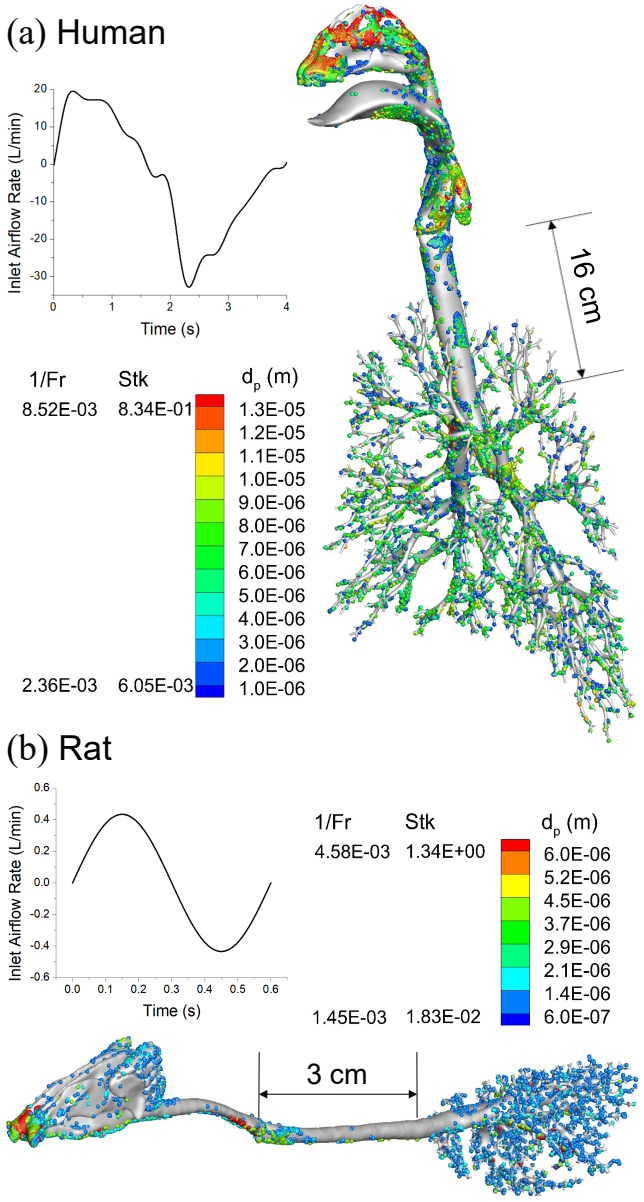

FIGURE 1. COMPARISONS OF PARTICLE DEPOSITION LOCATIONS IN HUMAN AND RAT RESPIRATORY SYSTEMS WITH TRANSIENT BREATHING WAVEFORMS FOR BOTH SPECIES AT REST: (A) HUMAN, AND (B) RAT

In the human nasal cavity, small microparticles with Stk≈8.34E-1 are able to enter the posterior of the nose, while the particles with the same Stk are mostly trapped in rat nasal vestibule (see Figs. 1 (a) and (b)). The deposition difference is

Downloaded from https://proceedings.asmedigitalcollection.asme.org/BIOMED/proceedings-pdf/DMD2020/83549/V001T07A005/6552792/v001t07a005-dmd2020-9060.pdf by guest on 28 July 2020

Copyright © 2020 ASME

due to the relatively narrower and more complex passages in the rat nose, which enhanced the chance for the particle deposition induced by inertial impaction and interception. Specifically, particles larger than 6 μm (Stk>1.34E+0) are mostly trapped in the front of the nasal cavity and not able to reach the olfactory region or the rat tracheobronchial tree. Therefore, in pre-clinical studies of pulmonary drug particles with the above-mentioned range of Stk, the rat airway model will not be available for the evaluation of drug delivery efficiency since no particles larger than 6 μm (Stk>1.34E+0) can reach the rat airways. In contrast, particles with Stk smaller than 6E-1 (1 μm <d_p<11 μm) and 2E-1 (0.6 μm <d_p<2 μm) in human and rat cases, respectively, can follow the air stream and successfully reach the TB trees. Particles with Stk from 1.8E-2 to 4.5E-2 (0.6 μm <d_p<1 μm) have the lowest deposition in the upper airway and trachea of the rat, and the resultant highest delivered dose in the TB tree of the rat.

2.3 Nondimensional Analysis of Particle Depositions

To study the effects of morphological and biological differences between rat and human airways on particle depositions, the variation of DF vs. Stk was investigated.

Based on its definition, Stk was calculated using the averaged inhalation flow rates and the nasal inlet hydraulic diameter (D_{in}) of both human and rat. The regional deposition fractions (DFs) changed with Stk are aligned with S-shape curves in both human and rat nasal cavity, which is in good agreement with the deposition data in the open literature [16]. The comparison also proves that the complexity of the rat respiratory system morphology, especially the nasal cavity, compared with that of the human respiratory system has a significant influence on different deposition patterns of inhaled drug particles that should not be neglected. However, using Stk as the independent variable is not able to make the DFs in human and rat respiratory systems to be uniformly aligned with a single curve. Furthermore, to observe how particle deposition is affected by gravitational force, how DFs varies with 1/Fr ($\sqrt{gd_p}/\mathrm{v}$) was also studied. Particles with the same 1/Fr did not have the same DF in between rat and human respiratory systems. Therefore, it is not available to predict the deposition of drug particles in the human airway from that in rat airway based on particle sedimentation mechanism.

Therefore, in order to establish the similarity between the particle depositions in human and rat respiratory systems, plotting DFs as a function of Stk or 1/Fr are not feasible. Instead, regional DFs of both species were plotted as a function of the ratio between Stk and Fr (i.e., Stk/Fr) (see Figs. 2 (a) and (b)). The ratio Stk/Fr is defined as:

$$\frac{Stk}{Fr} = \frac{\rho {d_p}^2 v}{18\mu D_{in}} \frac{\sqrt{g d_p}}{v} = \frac{\rho {d_p}^{2.5} g^{0.5}}{18\mu D_{in}} \tag{3}$$

Specifically, Fig. 2 (a) shows the DFs in the upper airway, i.e., from mouth/nose to the trachea, for particles with different Stk/Fr. Fig. 2 (b) displays the DFs in the tracheobronchial trees starting from G0. It is worth mentioning that since the human and rat respiratory systems are not complete and part of the small airways was truncated, an assumption was made to enable the prediction of the DFs in the whole tracheobronchial tree. Specifically, it is assumed that the escaped particles from the truncated airway outlets will deposit in the missing deeper airways and will not be exhaled and re-enter the airway domains for both the human and the rat.

It can be observed from Figs. 2 (a) and (b) that DFs in rat and human respiratory systems are aligned well as a function of Stk/Fr. The consistent trends of the DFs demonstrate that projecting the data from rat study to human study can be accurately done if Stk/Fr values of the particles are identical in between the human and the rat. Specifically, Figs. 2 (a) and (b) shows particles with the same value of Stk/Fr entering the human and rat airways through nostrils being carried by the airflow under resting condition would show the same qualitative deposition results in UA and TB. Equation (3) implies that the particle diameter, gravity, and, the inlet area of the nasal cavity are the key parameters to influence the DFs in both human and rat, which can be proved by Figs. 2 (a) and (b).

Employing the non-linear least-squares analysis, a piecewise correlation was generated for the DFs in the UA and trachea as a function of Stk/Fr for both human and rat, i.e.,

$$DF_{UA} = C_1 + C_2\, exp\left(C_3 \frac{Stk^{C_4}}{Fr} + C_5 \frac{Stk^{C_4-1}}{Fr}\right) \tag{4a}$$

where C_i (i=1 to 5) are coefficients, of which the values are dependent on Stk/Fr and given in Table 2. As it is plotted in Fig. 2, Eq. (4 a) can predict DFs in human and rat airways. Accordingly, the DFs in the TB tree can be given as:

$$\mathrm{DF}_{TB} = 1 - \mathrm{DF}_{UA} \tag{4b}$$

Using Eqs. 4 (a) and (b), the novel scale-up method between rat and human can be achieved by matching the value of Stk/Fr in the human and the rat.

TABLE 2. THE COEFFICIENT VALUES IN EQ. (4A)

	1.43E-5< $\frac{Stk}{Fr}$ <8.4E-5	8.4E-5< $\frac{Stk}{Fr}$ <6.7E-4	6.7E-4< $\frac{Stk}{Fr}$ <7E-3
C_1	2.70E-2	2.80E-2	1.92E-1
C_2	0.00E+0	2.70E-1	4.54E+0
C_3	1.26E+0	1.26E+0	-1.25E+1
C_4	1.8E-1	-7.80E-2	5.30E-1
C_5	1.4E-3	-7.00E-4	-8.54E-2
MSD	3.47E-07	6.62E-24	1.62E-4

It is worth mentioning that extrapolating particle DFs from rat study to human study is incorrect if RSA and RBW are used as the scale-up factors. In the last row of Table 2, the mean squared deviation (MSD) of the DF values are reported. MSD is defined as: :

$$MSD = \frac{1}{n}\sum_{i=1}^{n}(DF_i - \widehat{DF_i})^2 \tag{5}$$

in which $\widehat{DF_i}$ is obtained from Eq. (4), DF_i is from CFPD simulations, and n is the number of data points in each range of Stk/Fr. The overall MSD for all the data is 9.41E-5.

Downloaded from https://proceedings.asmedigitalcollection.asme.org/BIOMED/proceedings-pdf/DMD2020/83549/V001T07A005/6552792/v001t07a005-dmd2020-9060.pdf by guest on 28 July 2020

 Copyright © 2020 ASME

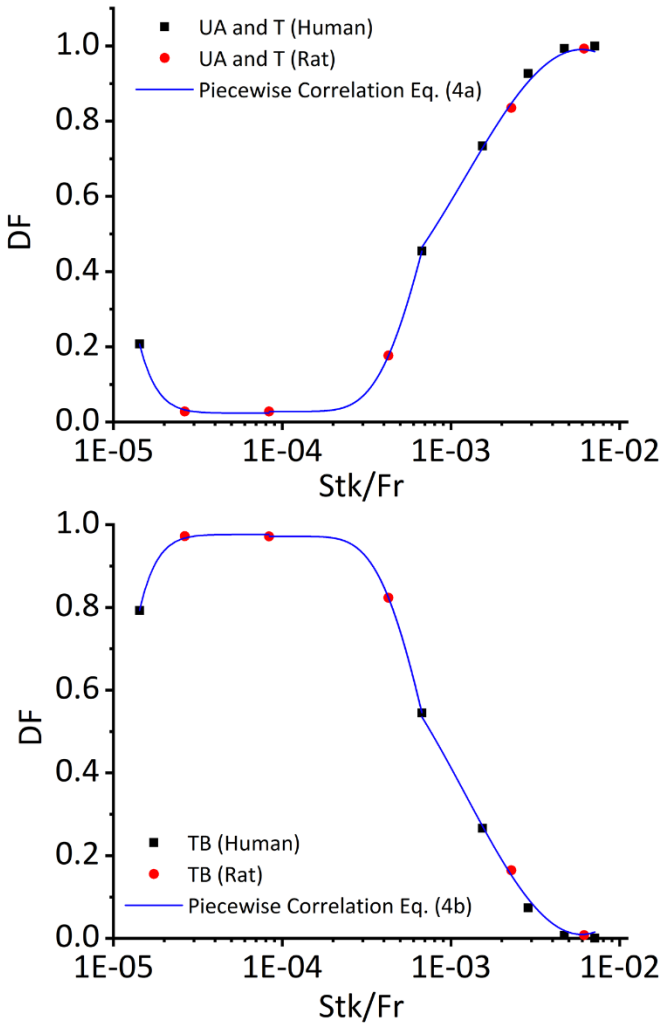

FIGURE 2. THE REGIONAL DEPOSITION FRACTIONS IN HUMAN AND RAT RESPIRATORY SYSTEMS AS A FUNCTION OF THE RATIO OF STOKES NUMBER TO FROUDE NUMBER: (A) THE DEPOSITION FRACTIONS IN THE MOUTH/NOSE-TO-TRACHEA REGIONS, AND (B) THE DEPOSITION FRACTIONS IN THE TRACHEOBRONCHIAL TREES

SUMMARY

A numerical inter-species study of particle transport and deposition in both human and rat respiratory systems was conducted using a CFPD modeling framework. Neglecting anatomical differences of the human respiratory systems between rats and humans leads to inaccuracies potentially. Numerical results demonstrate that existing extrapolations based on the ratios of airway surface areas or BW are not accurate. Incorporating the airway morphological effects, a unified correlation was generated to predict the regional particle depositions in both humans and rats as a function of a dimensionless number Stk/Fr. Using the correlation, projecting the preclinical rat study data of inhalable drug particles to human will be more accurate. Using the correlation (Eqs. 4 (a) and (b)) as the novel scale-up tool, inter-species extrapolations can be precisely done on predicting particle depositions in human respiratory systems based on the deposition data in rats obtained from animal studies. For future work, the precise scale-up method will be further extended using the *in silico* epidemiological study platform to extrapolate particle deposition and PK data from rat to human with statistical robustness and inter-subject variability studies.

The impact of the scale-up method in this study is broad, with many potential applications. For example, aerosolized toxic particles that are not soluble in water and smaller than 10 μm can reach lower airway and be irritant (or therapeutic). Being exposed to airborne phosgene ($COCl_2$) through insecticides and household substances) and oxides of nitrogen (through welding, fertilizers and air pollutants) can lead to asthma, airway edema, bronchiolitis obliterans, and other lower airway diseases [17]. Applying the "piecewise correlation equations" (see Eq. 4) can help scientists to utilize the delivered doses of pollutants in rat airway and to quickly evaluate the health risks to humans without clinical studies.

LIMITATIONS AND FUTURE WORK

Limitations of this study are listed as follows, which will be addressed in future work:

(1) Only nasal inhalation scenarios were simulated. The mouth inhalation cases will be simulated for both humans and rats in the future.

(2) Only solid particles with constant diameters were simulated in this study. The hygroscopic growth of inhalable droplets will be considered in future studies.

ACKNOWLEDGMENTS

This work was supported by the National Institute of General Medical Sciences of the National Institute of Health under Award Number P20GM103648. The use of ANSYS software (ANSYS Inc., Canonsburg, PA, USA) as part of the ANSYS-CBBL academic partnership agreement is gratefully acknowledged (Dr. Thierry Marchal, Global Industry Director). The authors are grateful for the supply of the rat data by Drs. R. Corley and A. Kuprat (Pacific Northwest National Laboratory).

REFERENCES

[1]R. F. Phalen, M. J. Oldham, and R. K. Wolff, "The relevance of animal models for aerosol studies," *Journal of Aerosol Medicine and Pulmonary Drug Delivery,* vol. 21, no. 1, pp. 113-124, 2008.

[2]G. D. Nielsen and I. K. Koponen, "Insulation fiber deposition in the airways of men and rats. A review of experimental and computational studies," *Regulatory Toxicology and Pharmacology,* vol. 94, pp. 252-270, 2018.

[3]J. Xi, J. Kim, X. A. Si, R. A. Corley, and Y. Zhou, "Modeling of inertial deposition in scaled models of rat and human nasal airways: Towards in vitro regional dosimetry in small animals," *Journal of Aerosol Science,* vol. 99, pp. 78-93, 2016.

Downloaded from https://proceedings.asmedigitalcollection.asme.org/BIOMED/proceedings-pdf/DMD2020/83549/V001T07A005/6552792/v001t07a005-dmd2020-9060.pdf by guest on 28 July 2020

Copyright © 2020 ASME

[4]C. Kleinstreuer, Z. Zhang, and C. S. Kim, "Combined inertial and gravitational deposition of microparticles in small model airways of a human respiratory system," *Journal of Aerosol Science,* vol. 38, no. 10, pp. 1047-1061, 2007.
[5]Y. Feng, Z. Xu, and A. Haghnegahdar, "Computational Fluid-Particle Dynamics Modeling for Unconventional Inhaled Aerosols in Human Respiratory Systems," *Aerosols-Science and Case Studies,* 2016.
[6]Y. Feng *et al.*, "An in silico inter-subject variability study of extra-thoracic morphology effects on inhaled particle transport and deposition," *Journal of Aerosol Science,* pp. 1-23, 2018.
[7]Z. Zhang, C. Kleinstreuer, and Y. Feng, "Vapor deposition during cigarette smoke inhalation in a subject-specific human airway model," *Journal of Aerosol Science,* vol. 53, pp. 40-60, 2012.
[8]R. A. Corley *et al.*, "Comparative computational modeling of airflows and vapor dosimetry in the respiratory tract of rat, monkey, and human," *Toxicological Sciences,* vol. 128(2), pp. 500-516, 2012.
[9]"ANSYS Fluent Theory Guide," no. Release 15.0, pp. 1-814, November 2013.
[10]D. C. Winter and R. M. Nerem, "Turbulence in pulsatile flows," *Annals of Biomedical Engineering,* journal article vol. 12, no. 4, pp. 357-369, July 01 1984.
[11]H. Hayati, A. S. Goharrizi, M. Salmanzadeh, and G. Ahmadi, "Numerical modeling of particle motion and deposition in turbulent wavy channel flows," *Scientia Iranica,* vol. 26, no. 4, pp. 2229-2240, 2019.
[12]P. G. Saffman, "The lift on a small sphere in a slow shear flow," *Journal of Fluid Mechanics,* vol. 22, no. 2, pp. 385-400, 1965.
[13]R. A. Corley *et al.*, "Comparative Risks of Aldehyde Constituents in Cigarette Smoke Using Transient Computational Fluid Dynamics/Physiologically Based Pharmacokinetic Models of the Rat and Human Respiratory Tracts," *Toxicological Sciences,* vol. 146, no. 1, pp. 65-88, 2015.
[14]C. E. Rennie, K. A. Gouder, D. J. Taylor, N. S. Tolley, R. C. Schroter, and D. J. Doorly, "Nasal inspiratory flow: at rest and sniffing," *Int Forum Allergy Rhinol* vol. 1, pp. 128–135, 2011.
[15]Y. Shang, J. Dong, K. Inthavong, and J. Tu, "Comparative numerical modeling of inhaled micron-sized particle deposition in human and rat nasal cavities," *Inhalation Toxicology,* vol. 27, no. 13, pp. 694-705, 2015.
[16]L. Nicolaou and T. A. Zaki, "Characterization of aerosol Stokes number in 90° bends and idealized extrathoracic airways," *Journal of Aerosol Science,* vol. 102, pp. 105-127, 2016.
[17]M. Gorguner and M. Akgun, "Acute Inhalation Injury," *Eurasian J Med.,* vol. 42, no. 1, pp. 28-35, 2010.

Downloaded from https://proceedings.asmedigitalcollection.asme.org/BIOMED/proceedings-pdf/DMD2020/83549/V001T07A005/6552792/v001t07a005-dmd2020-9060.pdf by guest on 28 July 2020

 Copyright © 2020 ASME